Clinical and Experimental Obstetrics & Gynecology

Clin. Exp. Obstet. Gynecol. **2026**; 53(7): 50127
https://doi.org/10.31083/CEOG50127

Original Research

Cyclophosphamide-Induced Ovarian Dysfunction Is Ameliorated by Lycopene by Targeting Reactive Oxygen Species-Mediated Cholesterol Metabolism Pathway

Shouye Ma[1], Xue Han[1], Yaping Pei[1], Xiaohong Chen[1], Huifang Wu[1], Mingjin Li[1,*]

[1]Department of Gynecology and Obstetrics, Gansu Provincial Hospital & The Third Hospital of Lanzhou University, 730000 Lanzhou, Gansu, China
*Correspondence: limingjin2000@163.com (Mingjin Li)

Academic Editor: Osamu Hiraike
Submitted: 18 January 2026 Revised: 27 February 2026 Accepted: 5 March 2026 Published: 1 July 2026

Abstract

Background: Premature ovarian failure (POF) refers to the loss of ovarian function in women younger than 40 years of age. Its incidence has increased annually, with a progressively younger age at onset. Women of reproductive age undergoing cancer treatments, such as radiotherapy and chemotherapy, may experience ovarian damage, leading to POF. Cyclophosphamide (CTX), a widely used chemotherapeutic agent, is a major cause of POF and severely compromises the reproductive health of female cancer survivors. However, the mechanism underlying CTX-induced ovarian damage remains not fully elucidated, and effective therapeutic strategies are lacking. **Methods:** Oxidative stress and cholesterol metabolism in ovarian tissues and cells following CTX treatment were assessed using enzyme-linked immunosorbent assay (ELISA), qRT-PCR, and Western blotting (WB). *In vitro* experiments were performed using mouse primary ovarian theca cells and granulosa cells to evaluate the impacts of CTX on oxidative stress and cholesterol metabolism, with the antioxidant lycopene (Lyc) administered as an interventional treatment. Additionally, *in vivo* therapeutic studies using Lyc were conducted to evaluate its regulatory effects on oxidative stress and cholesterol metabolism. **Results:** CTX triggers oxidative stress by enhancing reactive oxygen species (ROS) production and suppressing ROS clearance. CTX-induced ROS accumulation impairs cholesterol uptake and metabolic pathways. Specifically, CTX significantly downregulates the protein expression of low-density lipoprotein receptor (LDLR) and steroidogenic acute regulatory protein (StAR) in ovarian tissues and primary ovarian theca cells, leading to impairments in cholesterol transport and metabolism. Findings from both *in vitro* and *in vivo* assays showed that Lyc intervention markedly attenuates CTX-induced ROS accumulation, restores the expression of antioxidant enzymes and associated genes, and enhances the protein levels of LDLR and StAR in ovarian tissues and primary ovarian theca cells. **Conclusions:** CTX induces ovarian dysfunction by triggering ROS-mediated cholesterol metabolism disorders. Lyc exerts a protective effect against CTX-induced ovarian injury through its antioxidant activity, restoring cholesterol transport pathways and subsequent steroid hormone synthesis. Our findings provide a fresh mechanistic basis and a promising therapeutic strategy for preventing and treating chemotherapy-induced POF.

Keywords: lycopene; cyclophosphamide; premature ovarian failure; cholesterol metabolism; reactive oxygen species

1. Introduction

Premature ovarian failure (POF), marked by loss of ovarian function prior to the age of 40, is a devastating reproductive disorder affecting 1–4% of women of reproductive age [1]. Chemotherapeutic agents, particularly cyclophosphamide (CTX), are a leading cause of iatrogenic POF. CTX is a widely utilized agent for the treatment of multiple malignant tumors, among which are breast cancer, leukemia and lymphoma [2]. Over 30% of women younger than 35 years and 50% of women aged 35 to 40 years develop POF following chemotherapy; this condition lowers the likelihood of pregnancy in female cancer survivors by 40% compare with healthy counterparts [3]. CTX exerts ovarian toxicity mainly through two toxic metabolites: phosphoramide mustard and acrolein. Phosphoramide mustard induces follicle depletion and irreversible gamete damage, whereas acrolein impairs ovarian antioxidant defenses, increases free radical generation, and promotes oxidative stress, lipid peroxidation, and cellular injury [4]. However, its non-specific cytotoxicity causes irreversible damage to ovarian follicles and functional cells, leading to reduced estrogen secretion, infertility, and long-term complications such as osteoporosis [5]. Despite the clinical significance of CTX-induced ovarian injury, the underlying molecular mechanisms remain incompletely understood, and effective preventive or therapeutic interventions are still lacking.

Our previous studies have confirmed that CTX impairs ovarian cells by disrupting ovarian tissue inflammation, leading to dysregulated estrogen synthesis and ultimately POF [6]. In addition, CTX metabolism *in vivo* generates reactive oxygen species (ROS) that exceed the capacity of the cellular antioxidant defense system. Consequently, oxidative damage to lipids, proteins, and DNA in ovarian cells occurs, thereby leading to ovarian damage

[7]. However, the mechanisms underlying ovarian dysfunction and physiological abnormalities mediated by oxidative stress still require further investigation.

Cholesterol metabolism is essential for ovarian function, as cholesterol serves as a precursor for the biosynthesis of steroid hormones, including progesterone and estrogen [8]. The synthesis of steroid hormones in the ovary relies on the "two-cell, two-gonadotropin" model. Theca cells take up cholesterol from the circulation via the low-density lipoprotein receptor (LDLR), transport it to the mitochondria via steroidogenic acute regulatory protein (StAR), and synthesize androgens. Granulosa cells then convert androgens into estrogens through cytochrome P450 family 19 subfamily A member 1 (Cyp19a1) activity [9]. Disruption of any step in cholesterol metabolism can lead to insufficient steroid hormone synthesis and ovarian dysfunction [10]. Emerging evidence suggests that oxidative stress may interfere with cholesterol metabolism in various tissues [11], but whether this crosstalk contributes to CTX-induced ovarian injury has not been investigated.

Lycopene (Lyc), a natural lipophilic carotenoid primarily found in tomatoes and other red fruits, has gained attention for its potent anti-carcinogenic, antioxidant, and anti-inflammatory properties [12,13,14]. Previous studies have documented the beneficial effects of Lyc in numerous oxidative stress-related pathologies, including neurodegenerative diseases, cardiovascular diseases, and reproductive system lesions [15,16,17]. However, the potential protective effects of Lyc against CTX-induced ovarian dysfunction and its underlying mechanism, particularly its impact on cholesterol metabolism, remain unclear.

In the present study, we hypothesized that CTX-induced ROS accumulation disrupts cholesterol metabolism in ovarian cells, leading to insufficient steroid hormone synthesis and ovarian dysfunction, and that Lyc alleviates this injury by targeting ROS-mediated cholesterol metabolism pathways. To test this hypothesis, we established *in vivo* and *in vitro* models of CTX-induced ovarian injury and investigated the effects of Lyc on ROS levels, cholesterol metabolism-associated proteins, and steroid hormone synthesis. Our results provide new insights into the mechanisms underlying CTX-induced ovarian damage and support the potential application of Lyc as a promising intervention for chemotherapy-induced POF.

2. Materials and Methods

2.1 Animals and Treatments

Female C57BL/6 mice (7 weeks old, 16–20 g) were obtained from Shulaibao (Biotechnology Co., Ltd.; Wuhan, Hubei, China). Mice were housed to acclimate to the new environment for 1 week in a specific pathogen-free (SPF) environment under a 12-h light/dark cycle, controlled temperature (22 ± 2 °C) and humidity (50 ± 5%), with *ad libitum* access to food and water. All animal experiments were conducted in accordance with the National Institutes of Health (NIH) Guide for the Care and Use of Laboratory Animals (NIH Publication No. 80-23; revised 1978) and were approved by the Animal Experimental Ethical Inspection Committee of Guizhou Medical University (No. 2403436).

Inclusion criteria: Only intact female C57BL/6 mice aged 7 weeks with body weight ranging from 16 to 20 g, free of skin lesions, trauma and spontaneous organ diseases, were enrolled in this study. Exclusion criteria: Mice with abnormal growth, obvious wounds, abnormal food/water intake, or body weight fluctuation exceeding ±10% during the 1-week acclimation period were excluded prior to random grouping. Drug solvent and preparation conditions: Normal saline was used as the aqueous solvent for CTX and pentobarbital sodium; corn oil served as the lipid vehicle for Lyc. All working solutions were freshly prepared on the day of administration at room temperature under dim light. CTX powder was fully dissolved in sterile normal saline by gentle vortexing; Lyc powder was dissolved in corn oil via mild sonication to achieve complete dissolution without precipitation. All prepared drug solutions were discarded after daily dosing and were not stored for repeated use. In addition, all administrations used fixed dosing volumes: 10 mL/kg body weight for intraperitoneal injection and 5 mL/kg body weight for oral gavage.

After 1 week of acclimatization, mice were randomly allocated into 3 groups (N = 10 per group):

1. Vehicle (Veh) group: Mice received a single intraperitoneal injection of normal saline, as well as daily gavage with corn oil (vehicle for Lyc) for 21 consecutive days.

2. CTX group: Mice received a single intraperitoneal injection of CTX (100 mg/kg, Selleck, Cat. No. S1217, Houston, TX, USA) dissolved in normal saline, followed by daily gavage with corn oil for 21 consecutive days.

3. CTX + Lyc group: Mice received a single intraperitoneal injection of CTX (100 mg/kg), followed by daily gavage with Lyc (50 mg/kg, Selleck, Cat. No. S3943, Houston, TX, USA) dissolved in corn oil for 21 consecutive days.

Mice were anesthetized by intraperitoneal injection of 1% pentobarbital sodium (50 mg/kg). In accordance with Animal Research: Reporting of *In Vivo* Experiments (ARRIVE) guidelines and institutional animal care requirements, mice were euthanized by intraperitoneal administration of an overdose of 1% pentobarbital sodium (150 mg/kg). Death was confirmed by cessation of respiration and loss of the corneal reflex before tissue dissection.

2.2 Cell Culture

Primary mouse ovarian theca cells (Cat. No. CP-M205) and primary mouse ovarian granulosa cells (Cat. No. CP-M050) were obtained from Wuhan Procell Biotechnology Co., Ltd. (Wuhan, Hubei, China). Cells were maintained in the manufacturer-provided, cell type-specific

complete media (Cat. No. CM-M205 for theca cells; Cat. No.: CM-M050 for granulosa cells). All primary cells were validated for identity by surface marker analysis using quantitative real-time PCR PCR (qRT-PCR) and tested negative for mycoplasma contamination. Cells were plated into 96-well or 12-well plates and incubated at 37 °C in a humidified atmosphere with 5% CO_2. The culture medium was changed every 48 h to maintain optimal cell growth conditions.

2.3 Validation of CTX Stimulation and Lyc Treatment Concentrations

Primary mouse ovarian theca cells were seeded into 96-well plates at a density of 3000–5000 cells/well and stimulated with CTX at gradient concentrations of 0.1 μM, 0.15 μM, 0.2 μM, 0.25 μM, and 0.5 μM, followed by incubation for 24 h. After treatment, cell viability was assessed using a Cell Counting Kit-8 (CCK-8) assay kit (Cat. No. BS350B, Biosharp, Beijing, China) according to the manufacturer's instructions. Similarly, primary mouse ovarian theca cells were seeded in 96-well plates, stimulated with hydrogen peroxide (H_2O_2, 100 μM, CAS: 7722-84-1, Merck, Germany) as an oxidative stress positive control, and concurrently treated with Lyc at different concentrations (1 μM, 5 μM, 10 μM, 20 μM, 40 μM, and 100 μM). After 24 h of incubation, cell viability was measured using the CCK-8 assay kit to evaluate the cytoprotective effect of Lyc against oxidative stress-mediated cellular damage. In the present study, 0.2 μM CTX and 40 μM Lyc were finally selected as the optimal concentrations for subsequent *in vitro* cell treatment.

2.4 ROS Detection by Dihydroethidium (DHE) Staining

ROS levels in primary ovarian cells were assessed using DHE (Cat. No. 309800, Sigma-Aldrich, Darmstadt, Germany) staining. Briefly, cells were cultured on glass coverslips in 24-well plates and treated with 0.2 μM CTX and 100 μM H_2O_2. After the designated treatments, cells were cultured with 10 μM DHE at 37 °C for 30 min under light-protected conditions. The cells were then washed three times with phosphate-buffered saline (PBS), and nuclei were counterstained with DAPI (Cat. No, P0131, Beyotime, Shanghai, China) using anti-fade mounting medium. Coverslips were mounted onto glass slides, and images were acquired using a fluorescence microscope (Olympus, Tokyo, Japan). DHE fluorescence intensity was quantified using ImageJ software (1.54g version, National Institutes of Health, Bethesda, MD, USA).

2.5 Measurement of ROS Levels in Tissue and Cell Homogenates

ROS levels in mouse ovarian tissues and primary mouse ovarian theca cells were measured using a Tissue ROS Assay Kit (Cat. No. HR8821, BaiAoLaiBo, Beijing, China) according to the manufacturer's instructions. Briefly, PBS-washed ovarian tissues or scraped cells were collected into the homogenate buffer supplied with the kit and fully homogenized using a glass homogenizer. The homogenate was centrifuged at 100 ×g for 3 min at 4 °C, and the supernatant was collected. The ROS probe was then added, and samples were incubated at 37 °C for 15–30 min in the dark. Fluorescence intensity at 488 nm was measured using a microplate reader (MultiSkan, Thermo Fisher Scientific, Waltham, MA, USA).

2.6 Western Blot (WB) Analysis

WB was performed as previously described [18]. Total protein was extracted from ovarian tissues or primary ovarian cells using radioimmunoprecipitation assay (RIPA) lysis buffer (Cat. No. P0013D, Beyotime, Shanghai, China) supplemented with 1% phenylmethylsulfonyl fluoride (PMSF, Cat No. ST505, Beyotime, Shanghai, China) and 1% phosphatase inhibitor cocktail (Cat. No. P1081, Beyotime, Shanghai, China). Equal amounts of protein were resolved by 10% sodium dodecyl sulfate-polyacrylamide gel electrophoresis (SDS-PAGE) and transferred to polyvinylidene difluoride (PVDF) membranes (Millipore, Billerica, MA, USA). Membranes were blocked with 5% non-fat milk dissolved in tris-buffered saline with tween-20 (TBST) at room temperature for 2 h, and then incubated with primary antibodies overnight at 4 °C. The primary antibodies used were as follows: anti-LDLR (1:2000, Cat. No. 66414-1-Ig, Proteintech, Wuhan, Hubei, China), anti-StAR (1:2000, Cat. No. 12225-1-AP, Proteintech, Wuhan, Hubei, China), and anti-α-tubulin (1:1000, Cat. No. 80762-1-RR, Proteintech, Wuhan, Hubei, China). Membranes were washed three times with TBST, followed by incubation with horseradish peroxidase (HRP)-conjugated secondary antibodies at room temperature for 2 h. Protein bands were visualized using an enhanced chemiluminescence (ECL) detection kit (Cat. No. P0018S, Beyotime, Shanghai, China), and images were captured using a gel imaging system (Bio-Rad, Hercules, CA, USA). Relative protein expression levels were quantified using ImageJ software, with α-tubulin as the internal reference.

2.7 RNA Extraction and qRT-PCR

The protocol was performed as previously described [19]. Total RNA was extracted from ovarian tissues and primary ovarian cells using TRIzol® reagent (Cat. No. R0016, Beyotime, Shanghai, China). RNA purity and concentration were determined using a NanoDrop 2000 spectrophotometer (Thermo Fisher Scientific, Waltham, MA, USA). First-strand complementary DNA (cDNA) was synthesized using a HiScript II 1st Strand cDNA Synthesis Kit (+gDNA wiper) (Cat. No. R212-01, Vazyme, Nanjing, Jiangsu, China) according to the manufacturer's instructions. Quantitative RT-PCR (qRT-PCR) was conducted using the ChamQ™ SYBR® qPCR Master Mix (Cat. No. Q511-02, Vazyme, Nanjing, Jiangsu, China) on a StepOne-

Table 1. Primer sequences of genes.

Gene	Forward primer	Reverse primer
Idh1	AGTCCAGAGTGAAGAGGGTTATT	ATGGTAGCACACTTGACGCC
Sod1	CACTTCGAGCAGAAGGCAAG	CCCCATACTGATGGACGTGG
Sod2	AGGAGAGTTGCTGGAGGCTA	AGCGGAATAAGGCCTGTTGTT
Pex1	CACCTGCTGCAGAATCAAGC	ATCTGCTGAGAGAGGCTCCA
Ldlr	CCAATCGACTCACGGGTTCA	TCACACCAGTTCACCCCTCT
Star	GGAGCTCTCTGCTTGGTTCTC	CTTAGCACTTCGTCCCCGTT
Cyp17a1	GAGTTTGCCATCCCGAAGGA	TCTAAGAAGCGCTCAGGCAT
Cyp19a1	TCCACACTGTTGTGGGTGAC	AGGGAAGTACTCGAGCCTGT
Actin	TATAAAACCCGGCGGCGCA	TCATCCATGGCGAACTGGTG

Plus™ Real-Time PCR System (Applied Biosystems, Foster City, CA, USA). The relative expression levels of target genes were calculated using the $2^{-\Delta\Delta Ct}$ method, with Actin serving as the internal control to normalize gene expression across samples.

Primer sequences are listed in Table 1.

2.8 Kyoto Encyclopedia of Genes and Genomes (KEGG) Pathway Analysis of Differentially Expressed Genes (DEGs)

RNA sequencing data from ovarian tissues in mouse models of CTX-induced POF were obtained from the Gene Expression Omnibus (GEO, https://www.ncbi.nlm.nih.gov/gds/) under the accession ID GSE128240. For pathway enrichment analysis, the Database for Annotation, Visualization, and Integrated Discovery (DAVID, https://davidbioinformatics.nih.gov/) was utilized to conduct KEGG (https://www.genome.jp/kegg/) functional enrichment assays.

2.9 Histological Analysis of Ovarian Tissues

Ovarian samples were fixed with 4% paraformaldehyde for 24 h, dehydrated through graded ethanol solutions, embedded in paraffin, and sectioned at 5 µm thickness. Sections were deparaffinized, rehydrated, and stained with hematoxylin and eosin (H&E) for histological analysis. Images of ovarian sections were acquired using a light microscope (Olympus), and the ovarian structure was evaluated. Whole-section images and magnified views (100× and 200×) were used to evaluate the morphological changes in ovarian tissues.

2.10 Enzyme-Linked Immunosorbent Assay (ELISA) Analysis

ELISA kits were used to measure the concentrations of target analytes in ovarian tissue homogenates, serum samples, and cell supernatants, including superoxide dismutase (SOD, Cat. No. BC0170, Solarbio, Beijing, China), reduced glutathione (GSH, Cat. No. BC1175, Solarbio, Beijing, China), total cholesterol (TC, Cat. No. 60723ES60, Yeasen, Shanghai, China), low-density lipoprotein cholesterol (LDL-C, Cat. No. 60736ES59, Yeasen, Shanghai, China), progesterone (PRGE, Cat. No. EU0380, FineTest, Wuhan, Hubei, China), estradiol (E2; Solarbio Life Sciences, Cat. No. SEKM-0286, Beijing, China), ROS (ROS, Cat. No. HR8821, BaiAoLaiBo, Beijing, China), follicle-stimulating hormone (FSH; JONLNBIO, Cat. No. JL10239, Shanghai, China).

2.11 Statistical Analysis

All data are expressed as the mean ± standard error of the mean (SEM). Every N value shown throughout the manuscript corresponds to biological replicates for all experimental systems (including animal, cell and molecular experiments). Statistical analyses were conducted using GraphPad Prism 8.0 software (GraphPad Software, San Diego, CA, USA). For comparisons between two groups, differences were analyzed by an unpaired two-tailed Student's *t*-test. For comparisons among three or more groups, one-way or two-way analysis of variance (ANOVA) followed by Tukey's multiple comparison test was applied, as appropriate based on the number of independent variables. $p < 0.05$ was considered statistically significant.

3. Results

3.1 CTX Induces Oxidative Stress in Ovarian Tissue by Activating ROS Production and Inhibiting ROS Clearance

Our prior research revealed that CTX activates *p*-NF-κB/NLRP3/Caspase-1 signaling pathway, triggering aberrant inflammatory responses in ovarian tissues and identifying irisolidone as a potential therapeutic agent [6]. In addition to inducing inflammatory dysregulation, CTX also disrupts oxidative stress homeostasis in ovarian tissue. Thus, we aimed to further investigate the specific mechanisms by which CTX-induced oxidative stress modulates ovarian physiological functions, as well as to explore the potential of combination therapy with irisolidone and novel pharmacological agents for ovarian protection. To assess the overall impact of CTX on ROS levels in ovarian tissues, ovarian tissues were first homogenized, followed by ROS detection using a commercial assay kit. Findings demonstrated that ROS accumulation in ovarian samples from CTX-treated mice was significantly higher than that in the normal control group (Fig. 1A). Meanwhile, the activities of the ROS-

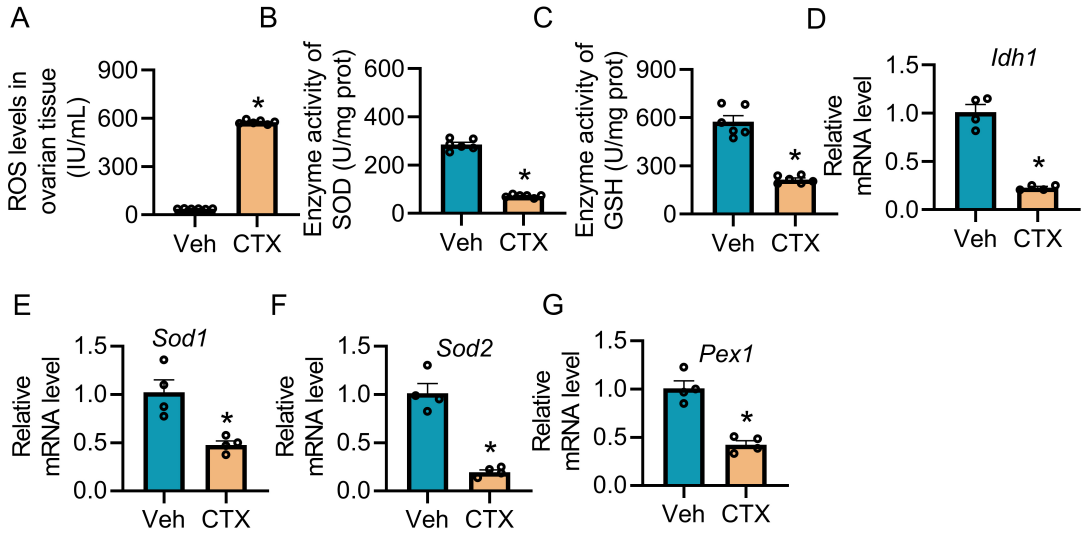

Fig. 1. CTX induces ROS production and inhibits ROS-scavenging capacity in ovarian tissues. (A) ROS levels in ovarian tissue homogenates were detected using a ROS assay kit (N = 6 per group). (B,C) The levels of antioxidant enzymes SOD (B) and GSH (C) in ovarian tissue homogenates were measured using ELISA kits (N = 6 per group). (D–G) The transcriptional expression levels of peroxisome-related genes in ovarian tissues, including *Idh1* (D), *Sod1* (E), *Sod2* (F), and *Pex1* (G), were assessed (N = 4 per group). Data are presented as mean ± SEM. Statistical analysis was performed using an unpaired Student's *t*-test. $p < 0.05$ was considered statistically significant, $^{*}p < 0.05$ vs. the vehicle group. CTX, cyclophosphamide; ROS, reactive oxygen species; SOD, superoxide dismutase; GSH, glutathione; ELISA, enzyme-linked immunosorbent assay; *Idh1*, isocitrate dehydrogenase 1; *Sod1*, superoxide dismutase 1; *Sod2*, superoxide dismutase 2; *Pex1*, peroxisomal biogenesis factor 1; SEM, standard error of the mean.

scavenging enzymes SOD and GSH were significantly inhibited by CTX (Fig. 1B,C). Additionally, the transcriptional expression of peroxisome-related genes, including isocitrate dehydrogenase 1 *(Idh1)*, superoxide dismutase 1 *(Sod1)*, superoxide dismutase 2 *(Sod2)*, and peroxisomal biogenesis factor 1 *(Pex1)*, was markedly downregulated in ovarian tissues following CTX treatment (Fig. 1D–G). Collectively, these findings indicate that CTX exposure increases ROS levels *in vivo* and impairs ROS-scavenging capacity, ultimately leading to ROS accumulation in ovarian tissues.

3.2 CTX Disrupts Cholesterol Metabolism Pathways in Ovarian Tissues

To investigate the biological processes affected by CTX in ovarian tissue, KEGG pathway enrichment analysis was performed on differentially expressed genes (DEGs) from CTX-induced ovarian tissue using the GSE128240 dataset. KEGG analysis of upregulated DEGs revealed that CTX affected the "hormone signaling" and "ovarian steroidogenesis" pathways (Fig. 2A). KEGG analysis of downregulated DEGs showed that CTX affected the "steroid biosynthesis", "fatty acid metabolism", and "cortisol synthesis and secretion" pathways in ovarian tissues (Fig. 2B). We hypothesized that CTX disrupts hormone synthesis processes in ovarian tissues.

Subsequently, we measured the concentration of TC and LDL-C in ovarian tissues, revealing a significant reduction in both parameters (Fig. 2C,D). In contrast, quantification of TC and LDL-C in serum demonstrated that CTX did not alter their circulating levels. This indicated that CTX impairs the ability of ovarian tissues to uptake free cholesterol and LDL-C (Fig. 2E,F). Therefore, we next examined the expression of LDLR, a key molecule for the uptake of circulating free cholesterol. The data demonstrated that CTX significantly suppressed LDLR expression (Fig. 2G,H).

3.3 CTX Inhibits Steroid Hormone Synthesis by Reducing Androgen Substrate Supply

After uptake of free cholesterol by ovarian theca cells, it is transported to the mitochondrial membrane to synthesize progesterone and androgens, which serve as direct substrates for estrogen synthesis in granulosa cells. We measured the concentrations of progesterone in ovarian tissues, and observed that CTX significantly reduced its level (Fig. 3A). We further examined the expression of StAR, a core protein responsible for transporting cytoplasmic cholesterol to the mitochondrial membrane, at both the transcriptional and protein levels. CTX stimulation caused a marked decrease in StAR expression in ovarian tissues (Fig. 3B,C). Previous studies have demonstrated that CTX remarkably inhibits the level of E_2 [6]. To fur-

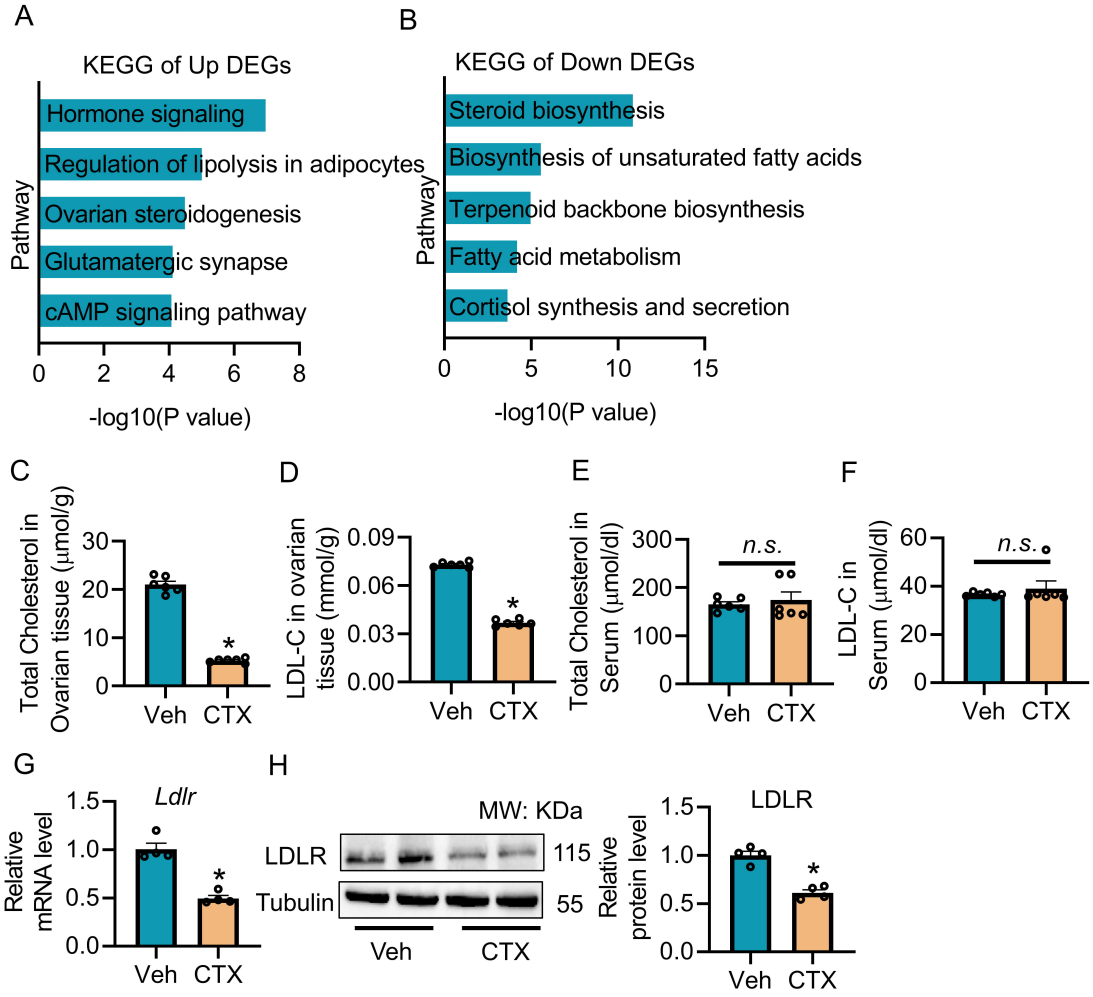

Fig. 2. CTX impairs cholesterol metabolism in ovarian tissues. (A,B) Gene expression profiles of ovarian tissues following CTX treatment were analyzed using the GSE128240. KEGG pathway analysis was performed on upregulated DEGs (A) and downregulated DEGs (B). (C,D) Levels of TC (C) and LDL-C (D) in ovarian tissue homogenates were measured by ELISA (N = 6 per group). (E,F) Levels of TC (E) and LDL-C (F) in serum were detected by ELISA (N = 6 per group). (G,H) The expression of LDLR in ovarian tissues was determined at the transcriptional level (G) and protein level (H) (N = 4 per group). Data are presented as mean ± SEM. Statistical analysis was performed using the unpaired Student's *t*-test. $p < 0.05$ was considered statistically significant, *$p < 0.05$ vs. the vehicle group, *n.s.* means no significant compared with vehicle group. KEGG, Kyoto Encyclopedia of Genes and Genomes; DEGs, differentially expressed genes; TC, total cholesterol; LDL-C, low-density lipoprotein cholesterol; LDLR, low-density lipoprotein receptor.

ther determine whether defects occur in the synthetic pathway from progesterone to estrogen, we assessed the expression of cytochrome p450 family 17 subfamily A member 1 (*CYP17A1*) and cytochrome p450 family 19 subfamily A member 1 (*CYP19A1*), key genes that regulate the conversion of progesterone to androgens and androgens to E_2, respectively. CTX stimulation significantly upregulated the transcriptional expression of *CYP17A1* and *CYP19A1* (Fig. 3D,E). We hypothesize that CTX does not impair the downstream enzymatic conversion of progesterone to androgens and estrogens; rather, it primarily disrupts cholesterol uptake and metabolism in ovarian tissues.

3.4 CTX Impairs Cholesterol Metabolism in Primary Ovarian Theca Cells

Primary mouse ovarian theca cells were treated with 0.2 μM CTX to establish an *in vitro* CTX stimulation model (Fig. 4A). Following CTX stimulation, cholesterol uptake and its subsequent conversion to progesterone were significantly impaired in ovarian theca cells (Fig. 4B,C). Furthermore, we investigated the effect of CTX stimulation on estrogen synthesis in granulosa cells cultured under androgen-free or androgen-supplemented conditions. Results demonstrated that, under normal conditions, estrogen synthesis in granulosa cells was markedly suppressed when cells were cultured in an androgen-free medium. In contrast, CTX stimulation did not inhibit estrogen synthesis in gran-

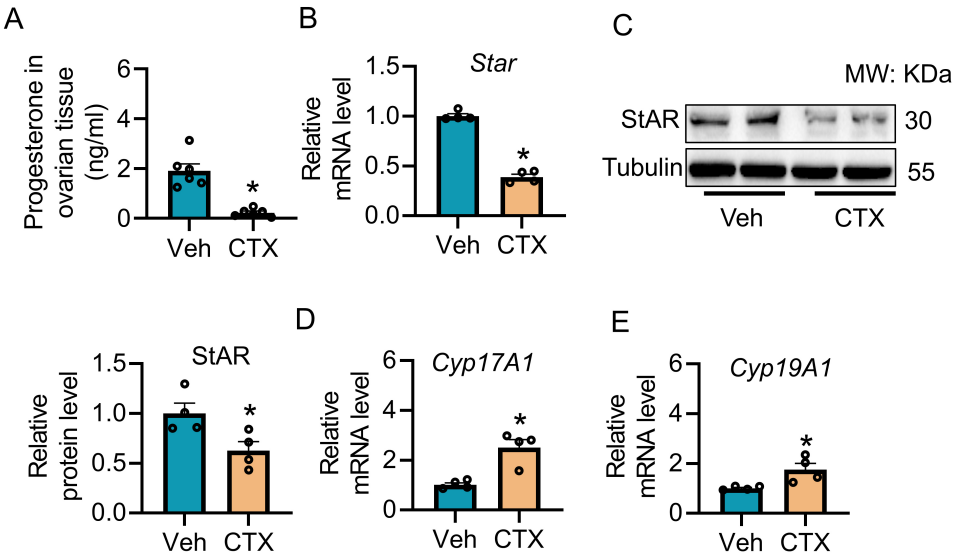

Fig. 3. CTX impairs the cholesterol metabolism processes in ovarian tissues. (A) The concentration of progesterone (a cholesterol metabolite) in ovarian tissue homogenates was detected by ELISA (N = 6 per group). (B,C) The expression of StAR, which mediates the transport of cytoplasmic cholesterol to mitochondria for metabolism, in ovarian tissues was detected at the transcriptional level (B) and protein level (C) (N = 4 per group). (D) The transcriptional expression of *Cyp17A1* in ovarian tissues was determined (N = 4 per group). (E) The transcriptional expression of *Cyp19A1* in ovarian tissues was determined (N = 4 per group). Values are expressed as mean ± SEM. Statistical comparisons were conducted via an unpaired Student's *t*-test. A *p*-value < 0.05 was considered statistically significant, **p* < 0.05 vs. the vehicle group. StAR, steroidogenic acute regulatory protein; *Cyp17A1*, Cytochrome P450 family 17 subfamily A member 1; *Cyp19A1*, Cytochrome P450 family 19 subfamily A member 1.

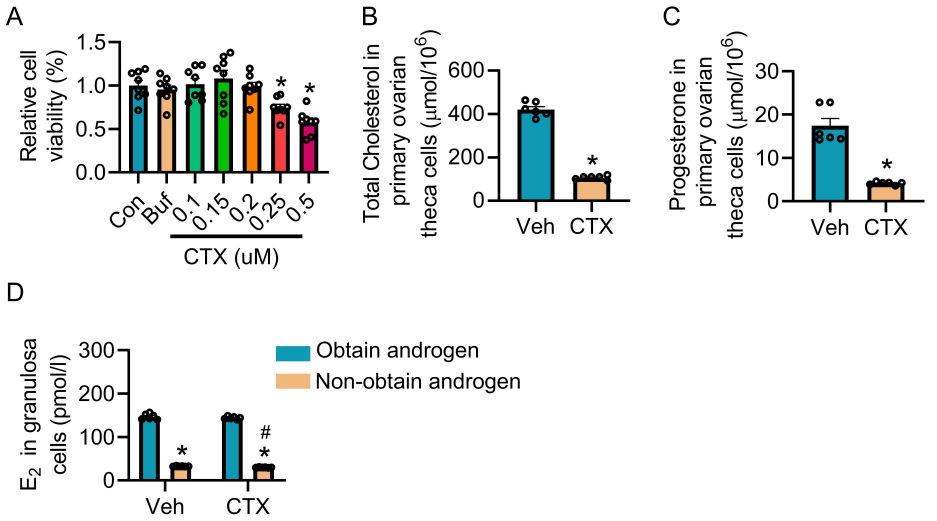

Fig. 4. CTX impairs cholesterol metabolism processes in mouse primary ovarian theca cells. (A) Cell viability following treatment with different concentrations of CTX in primary ovarian theca cells was performed using the CCK-8 assay (N = 8 per group). (B) Total cholesterol levels in ovarian theca cells were detected by ELISA (N = 6 per group). (C) progesterone levels in ovarian theca cells were detected by ELISA (N = 6 per group). (D) Primary granulosa cells were maintained in androgen-supplemented and androgen-free media, stimulated with CTX, and E_2 levels were determined by ELISA (N = 6 per group). Data are presented as mean ± SEM. Unpaired Student's *t*-test for two groups; one-way ANOVA with Tukey's post hoc test for multiple groups (one independent variable); two-way ANOVA with Tukey's post hoc test for multiple groups (two independent variables). $p < 0.05$ was considered statistically significant, *$p < 0.05$ vs. the corresponding control or vehicle group; $^{\#}$ $p < 0.05$ vs. the CTX-Obtain androgen group. CCK8, cell counting kit-8; E_2, estradiol; ANOVA, analysis of variance.

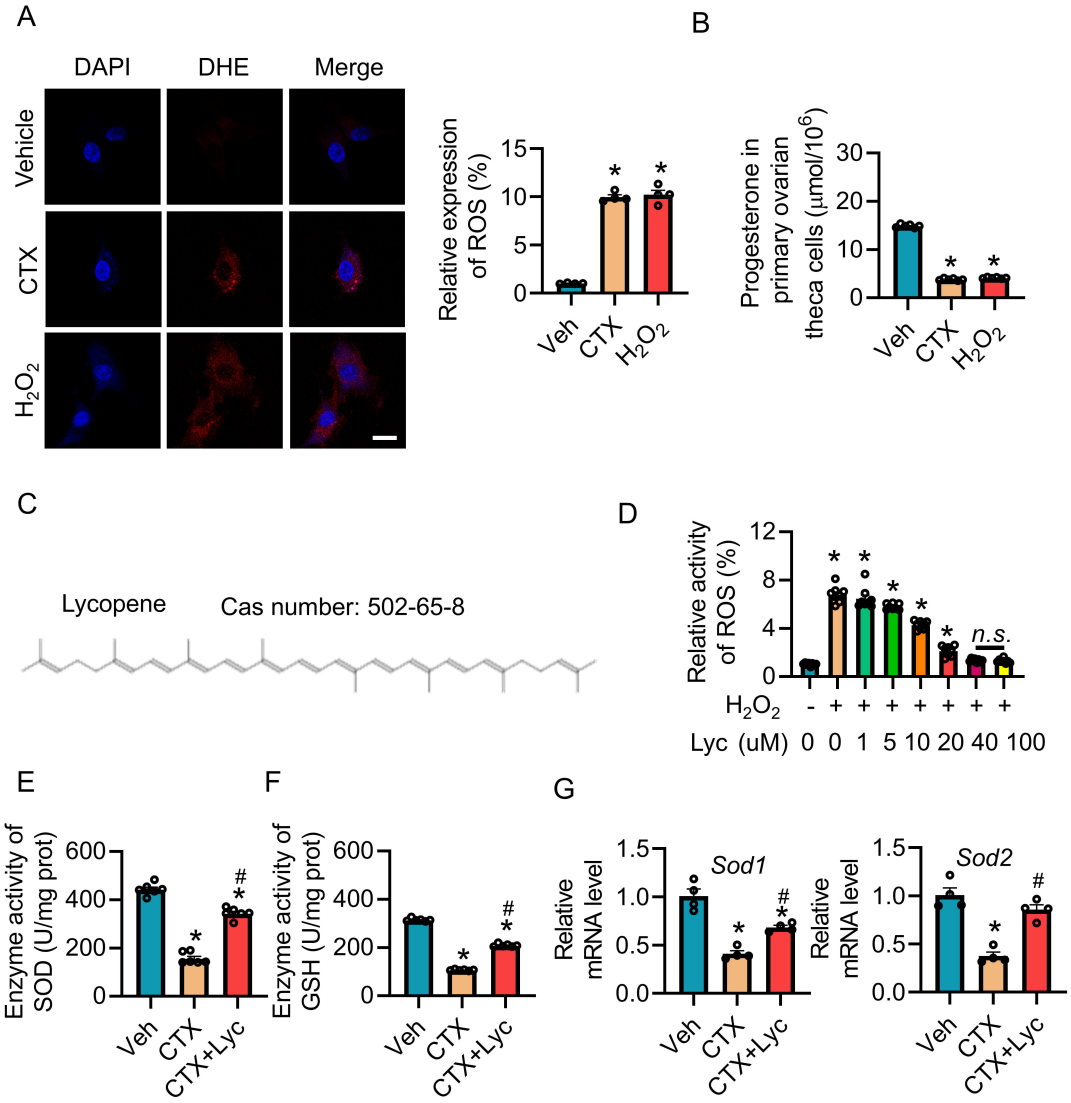

Fig. 5. Lyc attenuates CTX-induced ROS accumulation. Mouse primary ovarian theca cells were stimulated with CTX and H_2O_2 for 24 h. (A) ROS levels in theca cells after CTX and H_2O_2 stimulation were detected by DHE staining (N = 4 per group, scale bar = 50 μm). (B) progesterone levels in theca cells after CTX and H_2O_2 stimulation were measured by ELISA (N = 4 per group). (C) Chemical structure of Lyc. (D) Theca cells were stimulated with H_2O_2 followed by treatment with different concentrations of Lyc, and ROS levels were detected (N = 6 per group). (E,F) Theca cells were stimulated with CTX and then treated with Lyc; the enzymatic activities of SOD (E) and GSH (F) were detected by ELISA (N = 6 per group). (G) Theca cells were stimulated with CTX and then treated with Lyc; the transcriptional expression levels of *Sod1* and *Sod2* were detected (N = 4 per group). Values are expressed as mean ± SEM. One-way ANOVA with Tukey's post hoc test for multiple groups (one independent variable). $p < 0.05$ was considered statistically significant, *$p <$ 0.05 vs. the vehicle group; $^{\#}p < 0.05$ vs. the CTX group; *n.s.* means no significant compared with vehicle group. DHE, dihydroethidium; SOD, superoxide dismutase; Lyc, lycopene.

ulosa cells cultured in an androgen-supplemented medium (Fig. 4D). Collectively, these findings indicate that CTX impairs cholesterol uptake and metabolic processes in ovarian theca cells but does not compromise the ability of granulosa cells to utilize androgens as substrates for estrogen synthesis.

3.5 Lyc Inhibits CTX-Induced ROS Accumulation and Restores Antioxidant Enzyme Activity

Whether the inhibitory effect of CTX on cholesterol uptake and metabolism in ovarian theca cells is mediated by CTX-induced ROS remains to be further investigated. ROS staining of primary ovarian theca cells showed that CTX-induced ROS levels were comparable to those observed following direct stimulation with H_2O_2 (Fig. 5A). Both

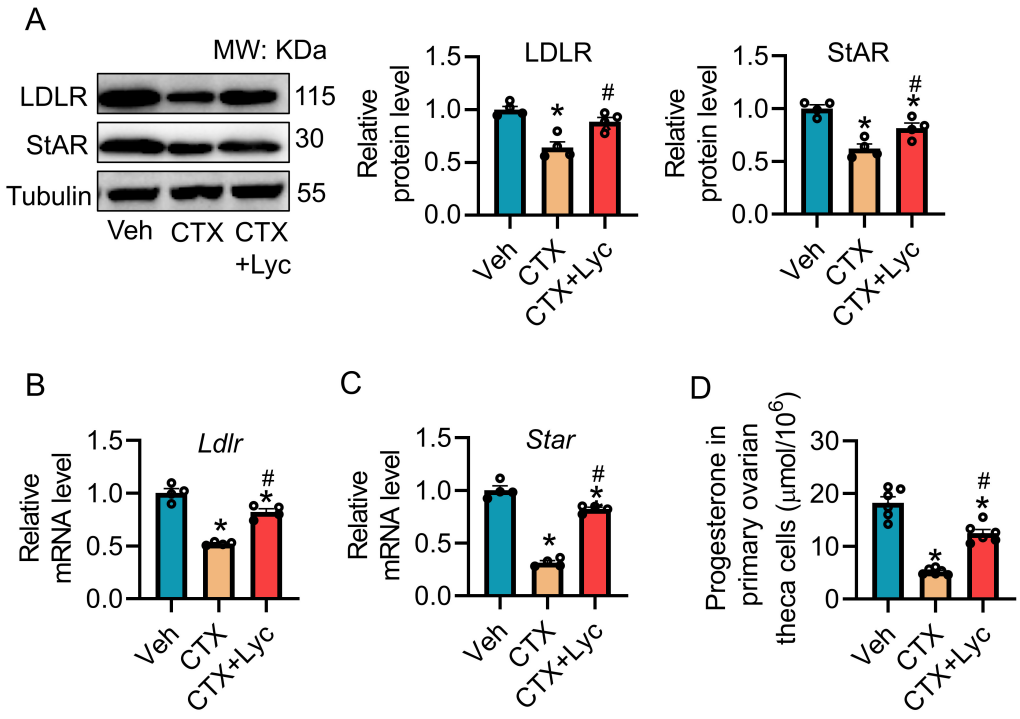

Fig. 6. Lyc ameliorates CTX-induced cholesterol metabolism disorder. (A–C) Primary ovarian theca cells were stimulated with CTX and then treated with Lyc; LDLR and StAR expression was assessed at the protein level (A) and transcriptional level (B,C) (N = 4 per group). (D) Primary ovarian theca cells were stimulated with CTX and then treated with Lyc; progesterone levels were measured by ELISA (N = 6 per group). Data are presented as mean ± SEM. One-way ANOVA with Tukey's post hoc test for multiple groups (one independent variable). $p < 0.05$ was considered statistically significant, $^{*}p < 0.05$ vs. the vehicle group; $^{\#}p < 0.05$ vs. the CTX group.

CTX and H_2O_2 inhibited progesterone synthesis (Fig. 5B). Therefore, we hypothesized that CTX-induced ROS disrupts cholesterol metabolism in ovarian theca cells. Based on the concept of homologous medicine and food, we selected Lyc to ameliorate CTX-induced damage in ovarian theca cells (Fig. 5C). Under H_2O_2 stimulation, 40 μM Lyc significantly scavenged H_2O_2-induced ROS accumulation (Fig. 5D). We further examined the ability of Lyc to restore antioxidant enzyme function and found that Lyc markedly reversed the CTX-induced decline in SOD and GSH enzymatic activities (Fig. 5E,F). Lyc also significantly upregulated the transcriptional expression of Sod1 and Sod2 (Fig. 5G). In conclusion, Lyc inhibits ROS accumulation and restores the activity and expression of antioxidant enzymes.

3.6 Lyc Restores CTX-Suppressed Cholesterol Uptake and Metabolism in Primary Ovarian Theca Cells

Although Lyc inhibits ROS accumulation, whether it can restore cholesterol uptake in ovarian theca cells remains to be investigated. We evaluated the effects of Lyc on LDLR and StAR expression in primary ovarian theca cells, and the findings demonstrated that Lyc notably reversed CTX-induced downregulation of LDLR and StAR at both transcriptional and protein levels (Fig. 6A–C). Additionally, the changes in progesterone levels demonstrated that Lyc treatment significantly restored progesterone synthesis compared with the CTX group (Fig. 6D).

3.7 Lyc Ameliorates CTX-Induced Ovarian Tissue Damage

To further verify whether Lyc ameliorates CTX-induced ovarian tissue damage *in vivo*, 8-week-old female mice were used. Mice received a single intraperitoneal injection of CTX (100 mg/kg). Based on previous literature, Lyc was administered by oral gavage at 50 mg/kg/day for 3 consecutive weeks (Fig. 7A) [20,21]. Relative to the control group, the CTX-stimulated mice showed a significant decrease in both body weight and ovarian weight; however, mice receiving Lyc displayed a notable recovery in ovarian weight and a marked rise in the ovarian index (ovarian weight/body weight ratio) (Fig. 7B–D). Morphological staining revealed that the Lyc treatment group exhibited a significant increase in the number of ovarian functional cells, including primordial follicle, primary follicle, secondary follicle, and antral follicle (Fig. 7E–I). In addition, the number of atretic follicles was significantly reduced (Fig. 7J). Collectively, these findings indicate that Lyc exerts a protective role against CTX-triggered injury in ovarian tissues.

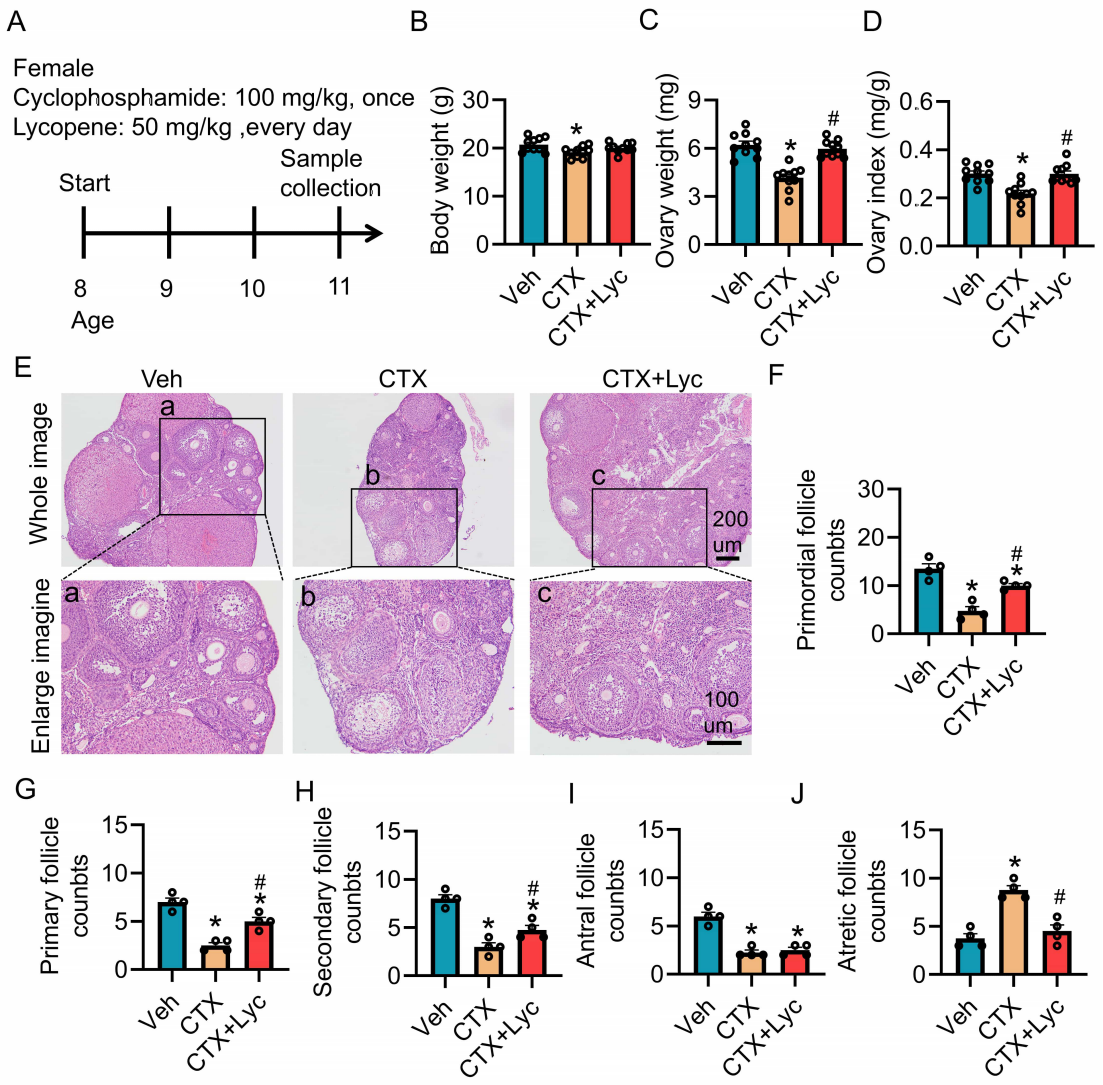

Fig. 7. Lyc ameliorates CTX-induced ovarian cell damage. (A) 8-week-old female mice were intraperitoneally injected with CTX (100 mg/kg) as a single dose, followed by intragastric administration of Lyc (50 mg/kg) daily for 3 consecutive weeks. (B) Body weights of mice in each group (N = 10 per group). (C) Ovarian weights of mice in each group (N = 10 per group).(D) Ovarian index of mice in each group (N = 10 per group). (E) H&E staining images of ovarian tissues in each group; the upper panels show the overview images (scale bar = 200 μm), and the lower panels show the magnified images of the black-boxed areas (scale bar = 100 μm; N = 4 per group). (F–J) Quantification of different ovarian cell types in ovarian tissues of each group, including primordial follicle (F), primary follicle (G), secondary follicle (H), antral follicle (I), and atretic follicle (J) (N = 4 per group). Data are presented as mean ± SEM. One-way ANOVA with Tukey's post hoc test for multiple groups (one independent variable). $p < 0.05$ was considered statistically significant, *$p < 0.05$ vs. the vehicle group; $^{\#}p < 0.05$ vs. the CTX group. H&E, hematoxylin and eosin.

3.8 Lyc Inhibits ROS Accumulation and Restores Estrogen Synthesis

Whether the therapeutic effect of Lyc is attributable to its potent antioxidant activity remains to be elucidated. ROS levels in mouse ovarian tissue homogenates were assessed, and the results showed that Lyc significantly inhibited CTX-induced ROS accumulation (Fig. 8A). Additionally, the concentrations of antioxidant enzymes (SOD and GSH) and the transcriptional levels of antioxidant genes (*Sod1* and *Sod2*) were assessed. Compared with the CTX-treated group, the Lyc-treated group markedly rescued SOD and GSH levels, and also significantly restored the transcriptional levels of *Sod1* and *Sod2* (Fig. 8B–E). We then explored whether the suppression of ROS by Lyc could restore cholesterol uptake and metabolism processes. Both the transcriptional and protein levels of LDLR and StAR were evaluated. Our findings revealed that Lyc treatment significantly restored the CTX-downregulated expression of LDLR and StAR at both examined levels (Fig. 8F–H). Impaired cholesterol uptake is known to disrupt estrogen

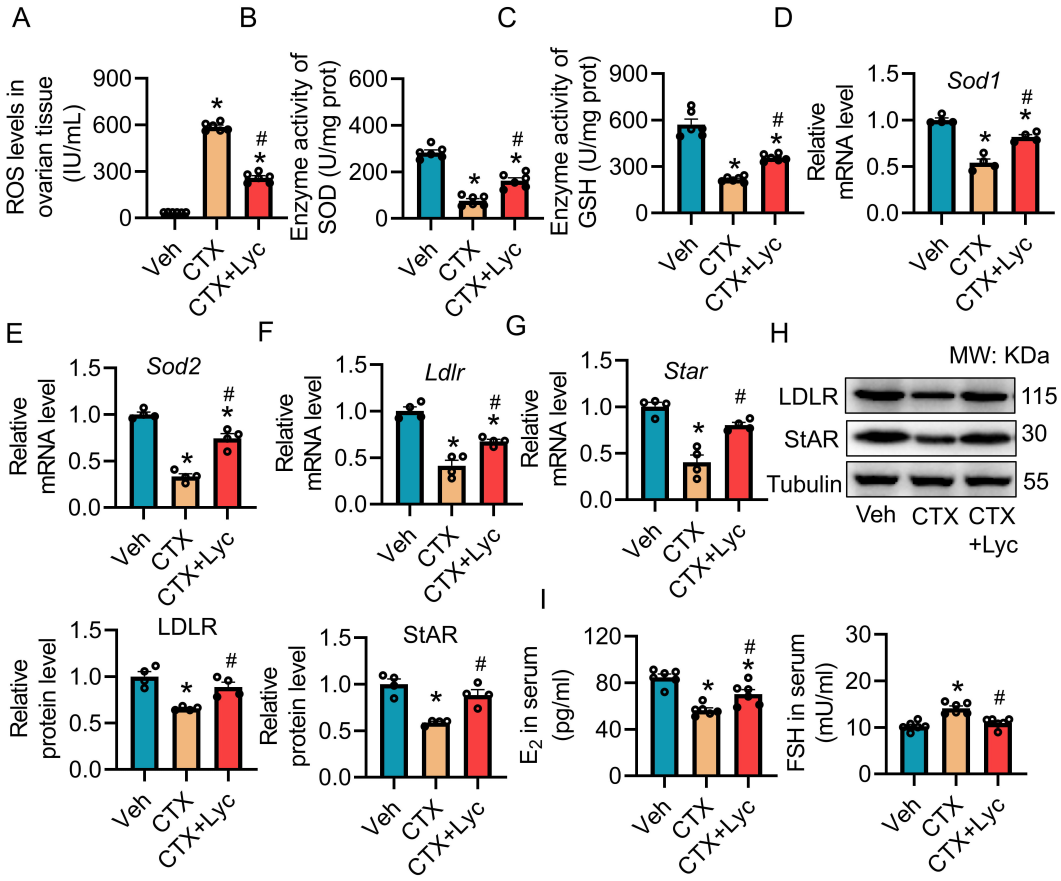

Fig. 8. Lyc inhibits CTX-induced ROS accumulation and restores cholesterol metabolism in ovarian tissues. (A) ROS levels in ovarian tissue homogenates of each group were detected using an ROS assay kit (N = 6 each group). (B,C) The enzymatic activities of SOD (B) and GSH (C) in ovarian tissue homogenates were measured by ELISA (N = 6 each group). (D,E) Transcriptional expression levels of *Sod1* (D) and *Sod2* (E) in ovarian tissues of each group were detected (N = 4 each group). (F,G) The transcriptional expression levels of *Ldlr* (F) and *Star* (G) in ovarian tissues of each group were detected (N = 4 each group). (H) Protein expression levels of LDLR and StAR in ovarian tissues of each group were detected (N = 4 each group). (I) Levels of E_2 and FSH in the serum of mice in each group were detected by ELISA (N = 6 each group). Data are presented as mean ± SEM. One-way ANOVA with Tukey's post hoc test for multiple groups (one independent variable). $p < 0.05$ was considered statistically significant, $^{*}p < 0.05$ vs. the vehicle group; $^{\#}p < 0.05$ vs. the CTX group. FSH, follicle-stimulating hormone.

synthesis. Thus, we further determined the levels of estrogen and FSH in serum. The data indicated that, compared with the CTX-treated group, Lyc treatment notably restored estrogen levels and reduced FSH levels (Fig. 8I). In conclusion, Lyc inhibits CTX-induced ROS accumulation, restores cholesterol uptake and metabolism in ovarian cells, and ultimately rescues estrogen synthesis.

4. Discussion

In the present study, we demonstrated that CTX induces ovarian dysfunction by triggering ROS-mediated disruption of cholesterol metabolism, and that Lyc exerts a protective effect by targeting this pathway. These findings provide new insights into the mechanism underlying CTX-induced ovarian injury and highlight the potential of Lyc as a therapeutic agent for chemotherapy-induced POF.

Consistent with previous studies, our findings demonstrated that CTX administration significantly increased ROS accumulation in primary ovarian cells [22]. Notably, CTX not only promoted ROS production but also reduced the expression of ROS-scavenging enzymes, SOD and GSH, leading to a self-amplifying cycle of oxidative stress. This dual effect of CTX on ROS homeostasis may explain its potent cytotoxicity in ovarian cells, which are highly sensitive to oxidative damage.

Cholesterol metabolism is critical to the synthesis of ovarian steroid hormones, and disruption of this process may lead to ovarian dysfunction [23]. KEGG pathway analysis indicated that DEGs affected by CTX were enriched in the cholesterol metabolism pathway. Further experiments confirmed that CTX downregulated two key proteins engaged in cholesterol uptake and mitochondrial transport,

namely LDLR and StAR. The CTX-induced downregulation of LDLR and StAR results in an insufficient supply of cholesterol required for steroid hormone synthesis, thereby impairing androgen and estrogen production. Furthermore, androgen supplementation partially restored estrogen synthesis in CTX-treated granulosa cells, which confirms that CTX-induced cholesterol metabolism disorder leads to androgen substrate deficiency and consequent reduced estrogen production.

Lyc is a natural antioxidant with multiple biological activities [24]. We found that Lyc suppresses CTX-induced ROS accumulation and upregulates the expression of *Sod1* and *Sod2*. This indicates that Lyc alleviates CTX-induced oxidative stress by enhancing the ROS scavenging system. Additionally, Lyc restored the expression of LDLR and StAR in CTX-treated ovarian cells, thereby reversing cholesterol metabolism disruption. Further animal experiments confirmed that Lyc attenuated CTX-induced morphological damage of ovarian tissues, supporting its protective effect on ovarian function.

Limitations

Several limitations of the present study should be acknowledged. First, this study examined the effects of Lyc on CTX-induced ovarian injury in mouse models only, suggesting that these findings may not be directly translatable to humans. Future studies should validate the protective effects of Lyc in human ovarian cells or in clinical trials. Second, the present work focused on the role of ROS-mediated disruption of cholesterol metabolism; however, additional mechanisms, such as apoptosis, may also contribute to CTX-induced ovarian injury, and the effects of Lyc on these mechanisms require further investigation. Third, a single dose of CTX (100 mg/kg) was administered to establish POF in mice, and the effects of Lyc on ovarian damage triggered by various CTX doses still require further investigation. Fourth, CTX did not affect estrogen synthesis in granulosa cells *in vitro* and increased the transcriptional expression of *CYP17A1* and *CYP19A1* in granulosa cells, suggesting that CTX does not impair granulosa cell function. However, H&E staining showed a significant reduction and structural disruption of granulosa cells. Therefore, the effects of CTX on granulosa cells require further experimental validation. Fifth, variations in estrous cycle stages among mice may influence their susceptibility to ovarian injury and compromise the assessment of hormone levels, as hormone concentrations inherently fluctuate across different estrous phases. Sixth, a variety of chemotherapeutic drugs are used clinically, not only CTX (an alkylating agent), and whether Lyc can protect the ovary from damage induced by other chemotherapeutic drugs remains to be further investigated.

5. Conclusions

In conclusion, this study demonstrates that CTX induces ovarian dysfunction by triggering ROS-mediated disruption of cholesterol metabolism, and that Lyc exerts a protective effect by scavenging ROS, restoring the antioxidant defense system, and reversing cholesterol metabolism and steroid hormone synthesis. These findings provide a novel theoretical basis for the prevention and treatment of chemotherapy-induced POF and highlight the potential of Lyc as a safe and effective therapeutic agent for this condition.

Availability of Data and Materials

All datasets utilized and analyzed in the present study are available from the corresponding author upon reasonable request. RNA sequencing data for the CTX-induced POF model were retrieved from the Gene Expression Omnibus (GEO) database under accession number GSE128240.

Author Contributions

MJL designed the study. SYM, XH, YPP, XHC, and HFW performed the experiments and collected data. MJL and SYM wrote the manuscript. All authors contributed to editorial changes in the manuscript. All authors read and approved the final manuscript. All authors have participated sufficiently in the work and agreed to be accountable for all aspects of the work.

Ethics Approval and Consent to Participate

All animal experiments were conducted according to the NIH guide for the care and use of laboratory animals (NIH Publication No. 80-23; revised 1978). All animal experiments were approved by the Ethics Committee at Guizhou Medical University (No. 2403436). All animal experiments were performed in accordance with the 3Rs principles (Replacement, Reduction and Refinement). We confirm the authenticity of this statement.

Acknowledgment

Not applicable.

Funding

This study was supported by the Research Fund Project of Gansu Provincial Hospital (24GSSYE-12) and Healthcare Research Project of Gansu Province (GSWSKY2022-17).

Conflicts of Interest

The authors declare no conflicts of interest.

Supplementary Material

Supplementary material associated with this article can be found, in the online version, at https://doi.org/10.31083/CEOG50127.

References

[1] Driscoll MA, Davis MC, Aiken LS, Yeung EW, Sterling EW, Vanderhoof V, et al. Psychosocial Vulnerability, Resilience Resources, and Coping with Infertility: A Longitudinal Model of Adjustment to Primary Ovarian Insufficiency. Annals of Behavioral Medicine : a Publication of the Society of Behavioral Medicine. 2016; 50: 272–284. https://doi.org/10.1007/s12160-015-9750-z

[2] Salman L, Covens A. Fertility Preservation in Cervical Cancer-Treatment Strategies and Indications. Current Oncology (Toronto, Ont.). 2024; 31: 296–306. https://doi.org/10.3390/curroncol31010019

[3] Stensheim H, Cvancarova M, Møller B, Fosså SD. Pregnancy after adolescent and adult cancer: a population-based matched cohort study. International Journal of Cancer. 2011; 129: 1225–1236. https://doi.org/10.1002/ijc.26045

[4] Khallaf WAI, Sharata EE, Attya ME, Rofaeil RR, Khalaf MM, Hemeida RAM, et al. Buspirone ameliorates premature ovarian insufficiency evoked by cyclophosphamide in female rats; attention to AMPK/Nrf2/HO-1, α-Klotho/NLRP3/Caspase-1, and Caspase-3-mediated apoptosis interplay. Toxicology and Applied Pharmacology. 2025; 500: 117373. https://doi.org/10.1016/j.taap.2025.117373

[5] Delahousse J, Molina L, Paci A. "Cyclophosphamide and analogues; a matter of dose and schedule for dual anticancer activities". Cancer Letters. 2024; 598: 217119. https://doi.org/10.1016/j.canlet.2024.217119

[6] Li M, Wei Z, Chen X, Wu H, Han X, Pei Y, et al. Irisolidone Ameliorates Cyclophosphamide-Induced POI via Inhibiting Inflammatory Response. Frontiers in Bioscience (Landmark Edition). 2025; 30: 45744. https://doi.org/10.31083/FBL45744

[7] Lu G, Li HX, Song ZW, Luo J, Fan YL, Yin YL, et al. Combination of bone marrow mesenchymal stem cells and moxibustion restores cyclophosphamide-induced premature ovarian insufficiency by improving mitochondrial function and regulating mitophagy. Stem Cell Research & Therapy. 2024; 15: 102. https://doi.org/10.1186/s13287-024-03709-0

[8] Lauridsen AR, Skorda A, Winther NI, Bay ML, Kallunki T. Why make it if you can take it: review on extracellular cholesterol uptake and its importance in breast and ovarian cancers. Journal of Experimental & Clinical Cancer Research : CR. 2024; 43: 254. https://doi.org/10.1186/s13046-024-03172-y

[9] Andersen CY, Ezcurra D. Human steroidogenesis: implications for controlled ovarian stimulation with exogenous gonadotropins. Reproductive Biology and Endocrinology : RB&E. 2014; 12: 128. https://doi.org/10.1186/1477-7827-12-128

[10] Liu X, Lv M, Zhang W, Zhan Q. Dysregulation of cholesterol metabolism in cancer progression. Oncogene. 2023; 42: 3289–3302. https://doi.org/10.1038/s41388-023-02836-x

[11] Li L, Guo Z, Zhao Y, Liang C, Zheng W, Tian W, et al. The impact of oxidative stress on abnormal lipid metabolism-mediated disease development. Archives of Biochemistry and Biophysics. 2025; 766: 110348. https://doi.org/10.1016/j.abb.2025.110348

[12] Leh HE, Lee LK. Lycopene: A Potent Antioxidant for the Amelioration of Type II Diabetes Mellitus. Molecules (Basel, Switzerland). 2022; 27: 2335. https://doi.org/10.3390/molecules27072335

[13] Kulawik A, Cielecka-Piontek J, Zalewski P. The Importance of Antioxidant Activity for the Health-Promoting Effect of Lycopene. Nutrients. 2023; 15: 3821. https://doi.org/10.3390/nu15173821

[14] Shih CM, Hsieh CK, Huang CY, Huang CY, Wang KH, Fong TH, et al. Lycopene Inhibit IMQ-Induced Psoriasis-Like Inflammation by Inhibiting ICAM-1 Production in Mice. Polymers. 2020; 12: 1521. https://doi.org/10.3390/polym12071521

[15] Przybylska S, Tokarczyk G. Lycopene in the Prevention of Cardiovascular Diseases. International Journal of Molecular Sciences. 2022; 23: 1957. https://doi.org/10.3390/ijms23041957

[16] Wang J, Li L, Li L, Shen Y, Qiu F. Lycopene alleviates age-related cognitive deficit via activating liver-brain fibroblast growth factor-21 signalling. Redox Biology. 2024; 77: 103363. https://doi.org/10.1016/j.redox.2024.103363

[17] Salem EA, Salem NA, Maarouf AM, Serefoglu EC, Hellstrom WJG. Selenium and lycopene attenuate cisplatin-induced testicular toxicity associated with oxidative stress in Wistar rats. Urology. 2012; 79: 1184.e1–6. https://doi.org/10.1016/j.urology.2011.12.006

[18] Mohyeldin RH, Sharata EE, Fawzy MA, Attya ME, Welson NN, Rofaeil RR. Memantine abrogates testicular dysfunction induced by risperidone in rats with a potential role of ERK1/2-Nrf2-caspase-3 signaling pathway. Scientific Reports. 2025; 15: 12914. https://doi.org/10.1038/s41598-025-94760-1

[19] Khalaf MM, Sharata EE, Khallaf WAI, Attya ME, Abo-Youssef AM, Hemeida RAM, et al. Buspirone combats cyclophosphamide-provoked hepatotoxicity in rats via activation of AMPK/Nrf2/HO-1 and suppression of NF-κB p65 /NLRP3 inflammasome pathways. Naunyn-Schmiedeberg's Archives of Pharmacology. 2026; 399: 5483–5498. https://doi.org/10.1007/s00210-025-04718-3

[20] Wu Y, Liu J. Functional food lycopene mitigates obesity-related cognitive decline via lipid metabolism regulation and neuroprotection via taurine and glutathione pathway. Clinical Nutrition (Edinburgh, Scotland). 2025; 51: 136–145. https://doi.org/10.1016/j.clnu.2025.06.005

[21] Liu X, Dilxat T, Shi Q, Qiu T, Lin J. The combination of nicotinamide mononucleotide and lycopene prevents cognitive impairment and attenuates oxidative damage in D-galactose induced aging models via Keap1-Nrf2 signaling. Gene. 2022; 822: 146348. https://doi.org/10.1016/j.gene.2022.146348

[22] Camp OG, Abu-Soud HM, Biernat MM, Chatzicharalampous C, Kofinas G, Kofinas JD. An updated look into reactive oxygen species and cyclophosphamide-induced ovarian damage. Journal of Ovarian Research. 2025; 18: 285. https://doi.org/10.1186/s13048-025-01849-2

[23] Cui D, Yu X, Guan Q, Shen Y, Liao J, Liu Y, et al. Cholesterol metabolism: molecular mechanisms, biological functions, diseases, and therapeutic targets. Molecular Biomedicine. 2025; 6: 72. https://doi.org/10.1186/s43556-025-00321-3

[24] Shafe MO, Gumede NM, Nyakudya TT, Chivandi E. Lycopene: A Potent Antioxidant with Multiple Health Benefits. Journal of Nutrition and Metabolism. 2024; 2024: 6252426. https://doi.org/10.1155/2024/6252426